International Journal of Mechanics, Energy Engineering and Applied Science(IJMEAS)
VOL. 3, NO. 2, May 2025, PP. 1-8
Print ISSN 3026-6815 | Online ISSN 3026-5673 | DOI prefix: 10.53893
https://journal.gpp.or.id/index.php/ijmeas/index

Using Finite Element Method to Calculate Strain Energy Release Rate, Stress Intensity Factor and Crack Propagation of an FGM Plate Based on Energy Methods

Huu-Dien Nguyen[1,*]
[1]Long An University of Economics and Industry, Vietnam

Email address:
nguyen.dien@daihoclongan.edu.vn
[*]Corresponding author

To cite this article:
Nguyen, H. (2025). Using Finite Element Method to Calculate Strain Energy Release Rate, Stress Intensity Factor and Crack Propagation of an FGM Plate Based on Energy Methods. *International Journal of Mechanics, Energy Engineering and Applied Science (IJMEAS), 3(2), 1–8. https://doi.org/10.53893/ijmeas.v3i2.395*.

Received: 03 21, 2025; **Accepted**: 05 28, 2025; **Published**: 05 30, 2025

Abstract: In the field of crack mechanics, predicting the direction of the crack when the propagation crack occurs is important because this will evaluate the crack when it propagates whether it penetrates into important areas, the danger of the structure or not. This paper will refer to three theories that predict the propagation direction of cracks: the theory of maximum tangential normal stress, the theory of maximum energy release and the theory of minimum strain energy density. At the same time, the finite element method (FEM)- ANSYS program will be used to calculate stress intensity factors (SIFs), strain energy release rate- J-integral, simulate stress field, displacement near a crack tip, and crack propagation phenomenon based on the above theories. The calculated results were compared with the results in other scientific papers and experimental results. This research used ANSYS program, an Experimental method combined with FEM based on the above energy theories to simulate J-integral, the SIFs and crack propagation. The errors of SIFs of a functionally-graded material (FGM)rectangular plate has a Internal Crack of 0.33% for K_I, 0.43% for K_{II}, the J-integral of 1.62% and crack propagation angle$\theta_c$of 0.15%. The FEM gave good errors compared to Experimental and Exactly methods.

Keywords: SIFs; FEM; FGM; J-Integral; Theory of minimum strain energy density; Theory of maximum energy release; Theory of maximum tangential normal stress.

1. Introduction

Functionally-graded material (FGM) is a new generation composite, which is applied in aeronautical engineering (engineering fuselage), in medicine (making teeth, artificial bones), in national defense (bulletproof armor), in energy industry (insulation panels, turbines, reactors).FGM material is a combination of two materials in which the volume ratio of each component changes smoothly and continuously [1].

In recent years, FEM is a numerical method that is widely used in mechanics to predict and model the mechanical behavior of structural materials. The FEM has emerged as an effective technique for analyzing crack problems. It is increasingly being used as a viable method in crack modeling that develops under the assumption of linear elastic fracture mechanics [2].

The SIF is an extremely important parameter in crack mechanics, indicating a degree of stress concentration at a crack tip. In three-dimensional space, the SIFsK_I, K_{II}, K_{III}, characterize the three independent displacements of a crack, including mode I, mode II, mode III. When predicting a propagation direction of two-dimensional cracks, the three energy methods $\sigma_{\theta\theta max}$, S_{min}, G_{max} all use two important parameters, K_I, K_{II}, to calculate the bending angle of the crack.

This paper will present the theories based on these methods and some simple propagation crack models referenced from other references. We use ANSYS software based on above three energy theories to calculate SIFs, strain energy release rate- J-integral, crack propagation angle θ_c of an FGM rectangular isotropic plate having a Through- thickness Center Crack and a Internal Crack. These mechanisms was also employed to check Experimental, the Exactly methods with calculated J-integral, SIFs and crack propagation phenomenon of a FGM rectangular isotropic plate.

2. Methods

2.1. The theory of maximum tangential normal stress $\sigma_{\theta\theta max}$

The mixed expressions of a elastic stress field around a crack tip when expressed in polar coordinates are as follows [3]:

$$\sigma_{rr} = \frac{1}{\sqrt{2\pi r}} cos\frac{\theta}{2}\left[K_I\left(1 + sin^2\frac{\theta}{2}\right) + \frac{3}{2}K_{II}sin\theta - 2K_{II}tan\frac{\theta}{2}\right] \quad (1)$$

$$\sigma_{\theta\theta} = \frac{1}{\sqrt{2\pi r}} cos\frac{\theta}{2}\left[K_I cos^2\frac{\theta}{2} - \frac{3}{2}K_{II}sin\theta\right] \quad (2)$$

$$\sigma_{r\theta} = \frac{1}{2\sqrt{2\pi r}} cos\frac{\theta}{2}\left[K_I sin\theta + K_{II}(3cos\theta - 1)\right] \quad (3)$$

In which, K_I, K_{II} are the two SIFs that characterize two independent displacement forms of the crack, which are mode I and mode II.

Theory of maximum tangential normal stress $\sigma_{\theta\theta max}$ first order for materials confirms that a crack will develop in the direction perpendicular to the theory of maximum tangential normal stress. This theory was proposed by Sih and Erdogan in 1963 [3] (see Fig. 1).

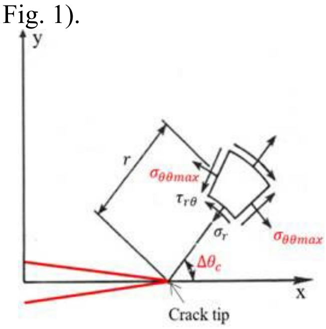

***Figure 1**. Maximum tangential normal stress in polar coordinate system.*

Derive equation (2) in terms of the variable θ and assign it to 0.

$$\frac{\partial\sigma_{\theta\theta}}{\partial\theta} = 0 \quad (4)$$

After rearranging and setting $\theta = \Delta\theta_c$, equation (2) will have the following form:

$$\frac{K_{II}}{K_I} = \frac{-\sin\Delta\theta_c}{3\cos\Delta\theta_c - 1} \quad (5)$$

Solving equation (5) according to the variable $\Delta\theta_c$, we will calculate the bending angle of the crack.

According to the reference from the reference [4], based on the theory of maximum tangential normal stress, the bending angle of the crack can also be calculated from the following formula:

$$\Delta\theta_c = \arccos\left[\frac{3K_{II}^2 + \sqrt{K_I^4 + 8K_I^2K_{II}^2}}{K_I^2 + 9K_{II}^2}\right] \quad (6)$$

In addition, the bending angle of the crack can also be calculated according to the reference formula from the reference [4] as follows:

$$\Delta\theta_c = 2\arctan\left[\frac{-2K_{II}/K_I}{1 + \sqrt{1 + 8\left(K_{II}/K_I\right)^2}}\right] \quad (7)$$

According to formula (7), if $K_{II} = 0$ then $\Delta\theta_c = 0$ (purely opening form (mode I only)). If $K_{II} > 0$, then the crack angle $\Delta\theta_c < 0$. If $K_{II} < 0$, then crack angle $\Delta\theta_c > 0$.

2.2. The theory of minimum strain energy density S_{min}

This theory was proposed by Sih in 1974 [5]. Sih developed the formula for calculating a strain energy density S according to stress intensity factors K_I, K_{II} as follows:

$$S = a_{11}K_I^2 + 2a_{12}K_IK_{II} + a_{22}K_{II}^2 \quad (8)$$

with

$$a_{11} = \frac{1}{16\mu}\left[(1 + cos\theta)(\kappa - cos\theta)\right] \quad (9)$$

$$a_{12} = \frac{1}{16\mu}sin\theta\left[2cos\theta - (\kappa - 1)\right] \quad (10)$$

$$a_{22} = \frac{1}{16\mu}\left[(\kappa + 1)(1 - cos\theta) + (1 + cos\theta)(3cos\theta - 1)\right] \quad (11)$$

where E is elastic modulus, ν is Poisson's ratio; shear module $\mu = \frac{E}{2(1+\nu)}$; $\kappa = \frac{3-\nu}{1+\nu}$ for plane stress; $\kappa = 3 - 4\nu$ for plane strain.

A crack will grow in a direction $\theta = \Delta\theta_c$, where the strain energy density is minimal.

$$\frac{dS}{d\theta} = 0 \text{ and } \frac{d^2S}{d\theta^2} > 0 \quad (12)$$

The crack starts to propagate when the strain energy density reaches its maximum value $S = S_{cr}$.

According to the reference from the document [6], the maximum value S_{cr} is calculated according to the following formula:

$$S_{cr} = (1 - 2\nu)(1 + \nu)K_{IC}^2 / 2E \quad (13)$$

where K_{IC} is the critical SIF.

2.3. Theory of maximum energy release G_{max}

This theory is based on the calculation of Hussain in 1974 [7]. These are the SIFs $\boldsymbol{K_I(\theta)}$ and $\boldsymbol{K_{II}(\theta)}$ of an initial major crack with a bending part with a very small angle $\boldsymbol{\theta}$ at the tip, calculated based on the SIFs $\boldsymbol{K_I}$ and $\boldsymbol{K_{II}}$ of normal cracks (see Fig. 2).

$$K_I(\theta) = g(\theta)\left(K_I\cos\theta + \frac{3}{2}K_{II}\sin\theta\right) \tag{14}$$

$$K_{II}(\theta) = g(\theta)\left(K_{II}\cos\theta - \frac{3}{2}K_I\sin\theta\right) \tag{15}$$

$$g(\theta) = \left(\frac{4}{3+\cos^2\theta}\right)\left(\frac{1-\theta/\pi}{1+\theta/\pi}\right)^{\frac{\theta}{2\pi}} \tag{16}$$

a)Original crack b)Kinked crack

***Figure 2**. Initial primary crack with a bending part with angle θ.*

According to Irwin's general expression [8], energy release rate G for the initial crack with a bent part with angle θ will be given as:

$$G(\theta) = \frac{1}{E'}\left(K_I^2(\theta) + K_{II}^2(\theta)\right) \tag{17}$$

with $E' = E$ for plane stress, $E' = \frac{E}{(1-\nu^2)}$ for plane strain.

Combined with equations (14), (15), (16), equation (17) becomes:

$$G(\theta) = \frac{1}{4E'}g'(\theta)\left[\left(1+3\cos^2\theta\right)K_I^2 - 8\sin\theta\cos\theta K_I K_{II} + \left(9-5\cos^2\theta\right)K_{II}^2\right] \tag{18}$$

The propagation angle of the crack is found by minimizing $G(\theta)$.

$$\frac{\partial G(\theta)}{\partial\theta} = 0 \tag{19}$$

And the following stability conditions must be satisfied:

$$\frac{\partial^2 G(\theta)}{\partial\theta^2} < 0 \tag{20}$$

The general form of equation (18) can be abbreviated as follows:

$$G(\theta) = \frac{1}{4E'}\left[A_{11}K_I^2(\theta) + A_{22}K_{II}^2(\theta) + 2A_{12}K_I(\theta)K_{II}(\theta)\right] \tag{21}$$

$$\begin{bmatrix} A_{11} \\ A_{12} \\ A_{22} \end{bmatrix} = g^2(\theta)\begin{bmatrix} 4-3\sin^2\theta \\ -2\sin 2\theta \\ 4+5\sin^2\theta \end{bmatrix} \tag{22}$$

2.4. Comparison between three methods of calculating crack propagation direction

The following is a formula comparing the results between the theory of maximum tangential normal stress with the theory of maximum energy release and the theory of minimum strain energy density as referenced from the references [9-12]. For the convenience of comparison, we put:

$$M^e = \frac{2}{\pi}\tan^{-1}\left(\frac{K_I}{K_{II}}\right) \tag{23}$$

In addition, this research would like to present another comparison between the three methods of calculating a propagation direction of the crack. This result is referenced from the literature [13].

Rice [14] and Eshel by [15] presented a contour integral encloses a crack front showed in Fig. 3:

$$J = \int_\Gamma \left(W dy - \vec{T}\frac{\partial\vec{\mu}}{\partial x}ds\right) \tag{24}$$

with J is the energy release rate (J/m^2); W is elastic strain energy density (J/m^3); $\vec{\mu}$ is the displacement vector at ds; n is the outward unit normal to Γ; ds is a differential element along the contour; $\vec{T}(\partial\vec{u}/\partial x)ds$ is input work; s is arc length; Γ is an arbitrary counterclockwise contour; $\vec{T}$ is the tension vector (traction forces) on the body bounded by Γ.

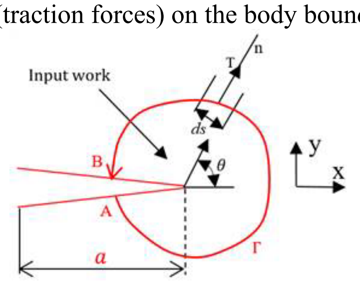

***Figure 3**. J-integral contours around the crack surfaces.*

Rice [14] and Riveros [16] certified a path independent concepts and found that stress energy release rate G is equal to J-integral:

$$J = G = \frac{K_I^2 + K_{II}^2}{E'} \tag{25}$$

where $E' = E$ for plane stress, $E' = \frac{E}{(1-\nu^2)}$ for plane strain.

3. Result and Discussions

An FGM plate with boundary conditions and dimensions was illustrated in Figure 4. The Poisson's ratio was determined to be $\nu = 0.25$, $a = 0.5$ cm, $H = 10$ cm, $W = 2$ cm, $\sigma = 10^6$N/m^2, and Young modulus E varied exponentially from left to right. Plane strain state was assumed.

$$E(x) = E_0 e^{\lambda x} \tag{26}$$

where $E_0 = 10^3$ Pa and $\lambda = 3$.

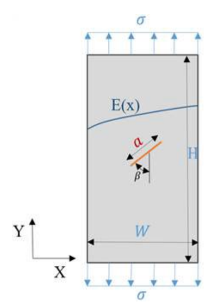

***Figure 4**. An Internal Crack model*

Experimental tests were conducted on a specimen with $H = 10$ cm, $W = 2$ cm, $a = 0.5$ cm, and thickness $t = 0.5$ cm which could be manufactured by the 3D printing. The material of specimen was nylon ABS with Poisson's ratio $v = 0.25$. The test samples were according to the ASTM E399 standard. A specimen was tested with different forces and speeds on an LF2373 Friction Tester machine. The specimen was tested with speeds v_1 ($v_1 = 3$ mm/min) for case 1; speeds v_2 ($v_2 = 4$ mm/min) for case 2. The load was applied $F = 100$ N for two cases (because value $F = \sigma/A$, with $A = Wt$ is the area of the specimen). A picture of Experimental setup is illustrated in Figure 5.

The displacement u_y are illustrated in Figure 6—by FEM with dimensions $H = 10$ cm, $a = 0.5$ cm, and $W = 2$ cm (see model Figure 4). Maximum displacements by the FEM Max(u_y) = 0.15638 (mm), by the Experiment for case 1 Max(u_y) = 0.16023 (mm), and % Error = 1.78%; case 2 Max(u_y) = 0.14861(mm), and % Error = 6.57% are as shown in Figure 6, Figure7 and Table 1. Figure 7 shows the curves stress- displacement of FEM and in two experiments, we see the stress Max(σ_{yy}) =1 Mpa (or 10^6 N/m^2) and three curses lie almost the same. Results illustrate that FEM is a reliable method when compared to Experimental method.

Results strain ε_y are illustrated in Figure 8—by FEM with the dimensions $H = 10$ cm, $a = 0.5$ cm, and $W = 2$ cm are similar to those of the model (Figure 4). The maximum strain by the FEM Max(ε_y) = 0.0015978 (mm/mm), by the Experiment for case 1 Max(ε_y) = 0.0016023 (mm/mm), and % Error = 0.57%; for case 2 Max(ε_y) = 0.0014861 (mm/mm), and % Error = 7.21% (Figure 8, Figure 9 and Table 1). Figure 9 shows the stress-strain curves of FEM and in two experiments, we see the stress Max(σ_{yy}) =1 Mpa (or 10^6N/m^2) and three curses lie almost the same. Results illustrate that FEM is a reliable method when compared Experimental method.

Results of delamination propagation y are illustrated in Figure 10—by FEM, and two case experiments. The maximum delamination propagation by the FEM Max(ε_y) = 0.1585 (mm), by the Experiment for case 1 Max(y) = 0.1602 (mm), and % Error = 1.06%%; for case 2 Max(y) = 0.1516 (mm), and % Error = 4.55%. Fig. 10 shows the curves of load-delamination propagation of FEM, and in two experiments, we see the load Max(F) = 100 N ($F = 10^6$ N/m^2/(2x0.5x10^{-4})m^2) and three curves lie on the same. Results illustrate that FEM is a reliable method.

Results of the FEM and two cases experiments show that the extension of crack length Δa of a FGM plate are illustrated in Figure 11. Maximum extension of crack length by the FEM at the time t =15(s) was Max(Δa) = 0.7116 (mm), by the Experiment for case 1 Max(Δa) = 0.7174 (mm), and % Error = 0.81%; for case 2 Max(Δa) = 0.7216 (mm), and % Error = 1.39%. Figure 11 shows the curves Extension of crack length - time of FEM, and in two experiments; the three curves lie the same. The results show that the FEM is a reliable method when compared to the Experimental method.

Table 1. *Comparison of the maximum displacement and strain between Experimental method and FEM*

	Displacement u_y(mm)	Strain ε_y(mm/mm)
FEM	0.15638	0.0015978
Experimental 1	0.16023	0.0016023
Experiment 2	0.14861	0.0014861
Error 1(%)	1.78	0.57
Error 2(%)	6.57	7.21

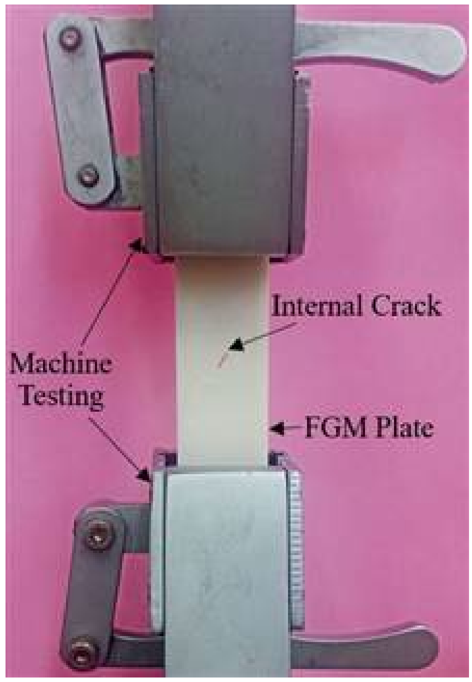

Figure 5. *The experimental setup.*

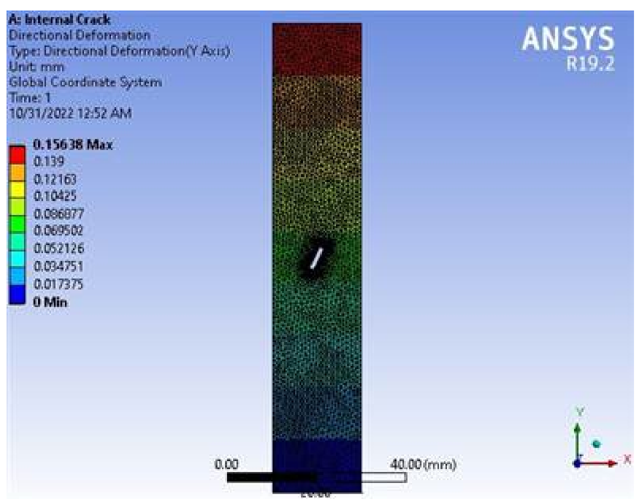

Figure 6. *The results of displacement u_y*

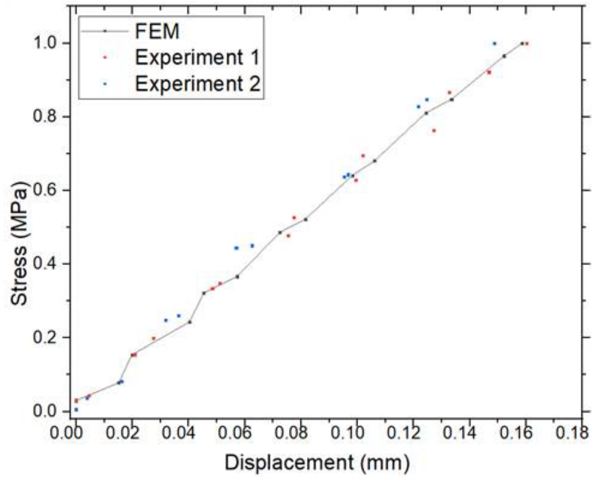

***Figure 7**. Comparison of modeling of displacement u_y of Experimental results and FEM*

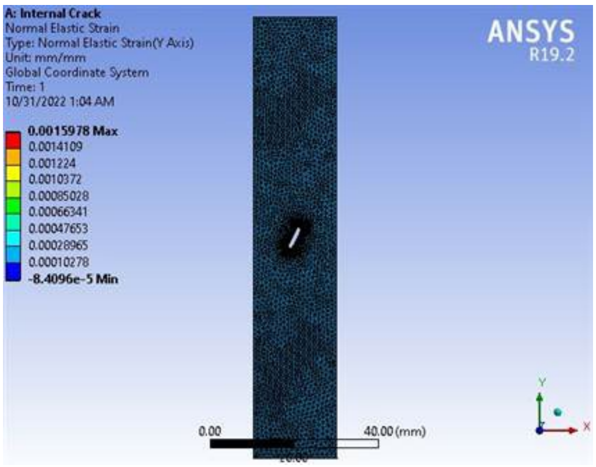

***Figure 8**. The results of strain ε_y*

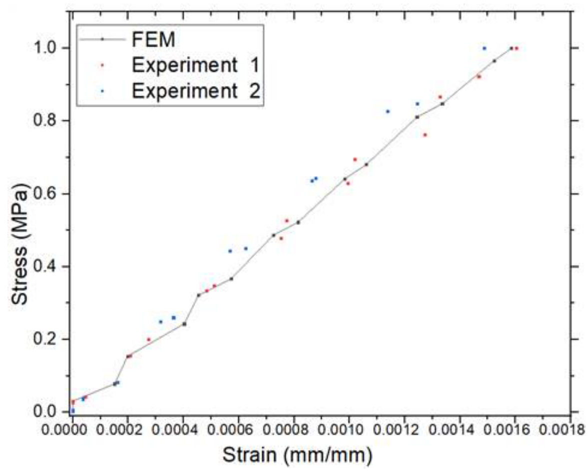

***Figure 9**. Comparison of modeling of strain ε_y of Experimental results and FEM*

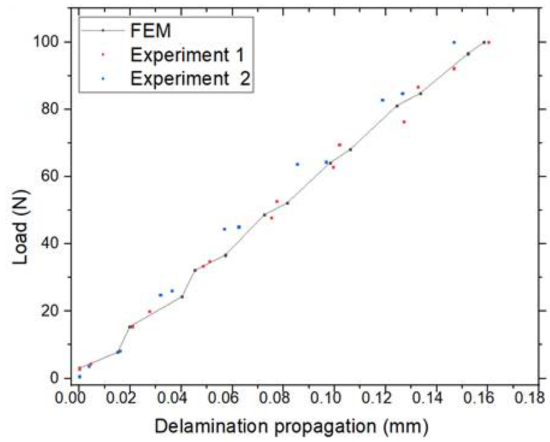

***Figure 10**. Comparison of delamination propagation y of Experimental results and FEM*

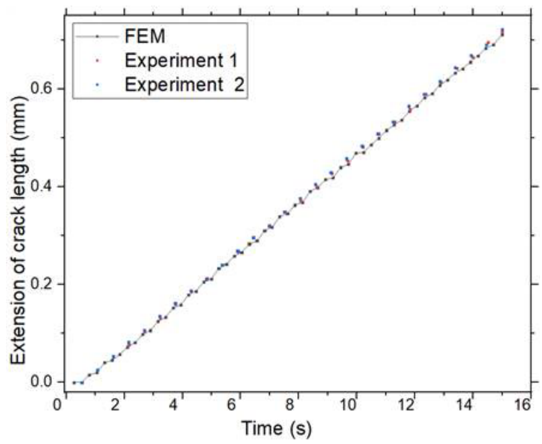

***Figure 11**. Comparison of extension of crack length Δa of FEM and experimental results*

Results of SIF analysis are Ref.[11] (with this model: $W = 2$ cm, $\sigma = 10^6$ N/m², $a = 0.5$ cm, $\beta = 60°$) as follows:

$$K_I = \sigma\sqrt{\pi a}\sin^2\beta = 0.3682 \text{ MPa}\sqrt{mm} \quad (27)$$

$$K_{II} = \sigma\sqrt{\pi a}\sin\beta\cos\beta = 1.1506 \text{ MPa}\sqrt{mm} \quad (28)$$

From equation (25), we got:

$$E' = \frac{E}{\left(1-\nu^2\right)} = 1009.0817 \text{ Pa} \quad (29)$$

$$J = \frac{K_I^2 + K_{II}^2}{E'} = 0.0014 \text{ mJ/mm}^2 \quad (30)$$

***Table 2.** Comparison of SIFs K_I, K_{II} between Exactly method and FEM*

SIFs	K_I	K_{II}
Exactly (MPa.$\sqrt{mm}$)	0.36820	1.1506
FEM (MPa.$\sqrt{mm}$)	0.36698	1.1501
Error (%)	0.33	0.43

The SIFs K_I are illustrated in Figure 12. SIFs K_I by the FEM $K_I = 0.36698$ (MPa.$\sqrt{mm}$), by the Exactly method $K_I = 0.3682$ (Mpa. $\sqrt{mm}$), and % Error K_I by FEM compared to Exactly method: Error_{FEM} =1.33% (Table 2). Figure 13 compares the curves SIFs versus crack length of FEM, exactly method and other reference results; the six curves lie the same. Results illustrate FEM is a reliable method.

Table 3. *Comparison of J-integral between FEM and Exactly method*

Exactly (mJ/mm^2)	0.001400
FEM (mJ/mm^2)	0.001423
Error (%)	1.62

The SIFs K_{II} are illustrated in Figure 14. SIFs K_I by the FEM K_{II} = 1.1501 (MPa.$\sqrt{mm}$), by the Exactly method K_{II} = 1.1506 (Mpa. $\sqrt{mm}$), and % Error K_I by FEM compared to Exactly method: Error_{FEM} =0.43% (Table 2). Figure 15 compares the curves SIFs versus crack length of FEM, exactly method and other reference results; the six curves lie the same. Results illustrate FEM is a reliable method.

The results J-integral are shown in Figure 16—by FEM and the Exactly method (in Equation 30). J-integral by the FEM J =0.001423 (mJ/mm^2), by the Exactly method J= 0.0014 (mJ/mm^2), and %Error J by the FEM compared to the Exactly method: Error = 1.62% (Table 3). Figure 17 compares the curves J-integral versus crack length of FEM, exactly method and other reference results; the six curves lie the same. Results illustrate FEM is is a reliable method.

The results M^e (see Equation 23) and θ_c (see Equation 7) are shown in Figure 18—by the FEM, Exactly and reference energy methods. M^e by FEM M^e = 0.31, by Exactly method M^e = 0.32; %Error M^e by FEM compared to Exact method: Error = 3.12%; Values θ_c by FEM θ_c = -64.5°, by Exactly method θ = -64.6°; %Error θ_c by FEM compared to Exact method: Error = 0.15% (Table 4). Because values $K_{II} > 0$ so values $\theta_c < 0$ – by theory (Equation 7). Figure 18 compares the curves θ_c versus M^e of FEM, Exactly method and reference energy methods; the five curves lie the same. The values M^e calculated at each step according to the three theories are approximately equal to 1 (between $0 - 1$). Therefore, the bending angle of the crack calculated according to the three theories at each step has nearly equal values. This is consistent with the graph comparing the results between the three theories that predict the propagation direction of the crack referenced from the literatures. Therefore, the crack path modeled according to the three theories has almost the same form. Results illustrate FEM is a reliable method.

Table 4. *Comparison of the* M^e *and* θ_c *between Exactly method and FEM*

	M^e	θ_c(degree)
Exactly	0.32	-64.6
FEM	0.31	-64.5
Error (%)	3.12	0.15

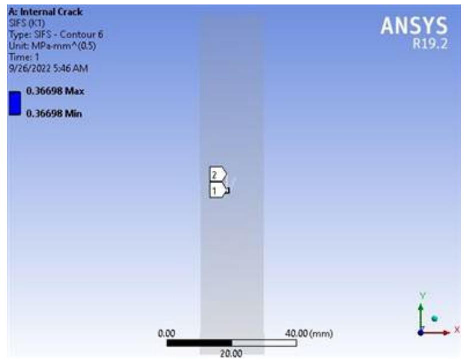

Figure 12. *The result of SIF* K_I

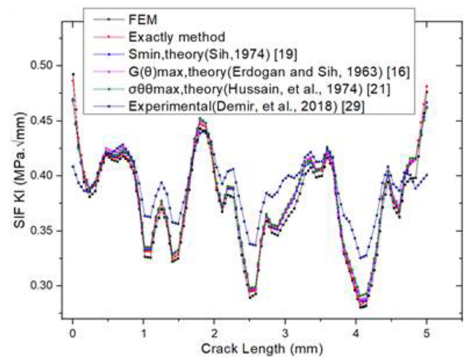

Figure 13. *Comparison of SIFs* K_I *versus crack length of FEM, exactly and other reference results*

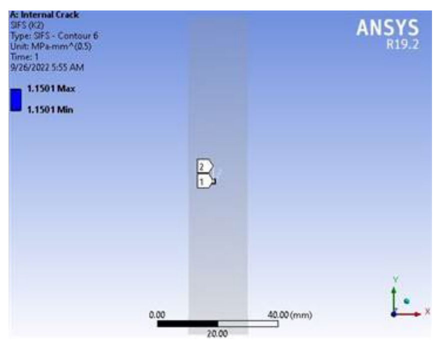

Figure 14. *The result of SIF* K_{II}

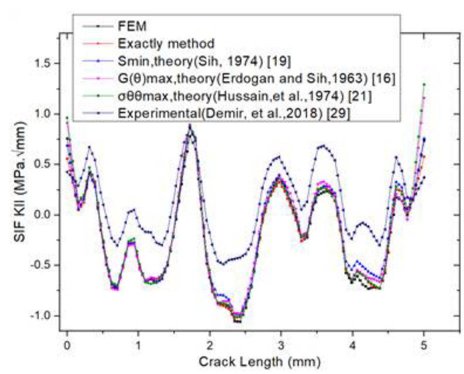

Figure 15. *Comparison of SIFs* K_{II} *versus crack length of FEM, exactly and other reference results*

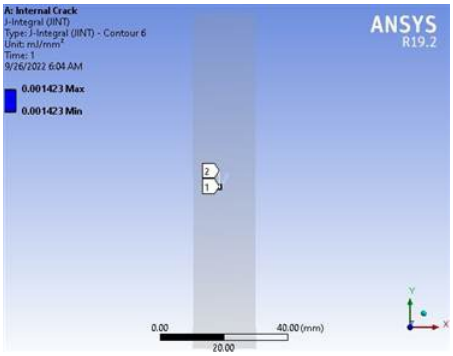

Figure 16*. The result of J-integral*

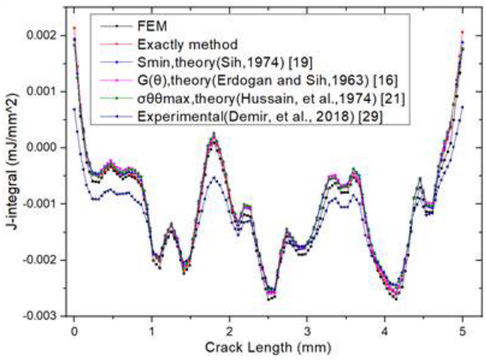

Figure 17*. Comparison of J-integral versus crack length of FEM, exactly and other reference results*

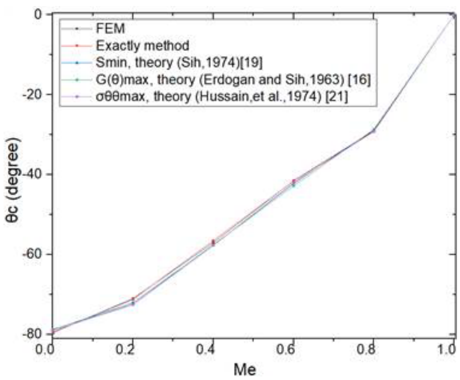

Figure 18. Comparison of modeling of $\theta_c$versus $M^e$of FEM, exactly and reference energy methods

4. Conclusion

In this research, we use FEM to simulate the crack tip behavior in two dimensions, and stress, displacement fields near a crack tip could be more exactly instead compared with experimental method. The calculation of the SIFs and J-integral will be faster than the analytical theory when encountering a complex crack model. Concurrently, it was possible to relatively calculate the growth and shape of the two-dimensional crack as it propagates under different conditions of the model, material, and loading method.

The SIFs, J-integral and crack propagation angle of the two cases mentioned in section 3 were calculated based on three energy methods. The results obtained by FEM were better than those obtained by Experimental method, when compared to Exactly method. These findings can be introduced as a new approach t calculate SIFs, J-integral and crack propagation phenomenon of the FGM plate.

Further, this research presented the FEM based on above three energy methods to calculate the SIFs, J-integral and crack propagation phenomenon of the FGM plate based on the reference models. These mechanisms are popular application in industrial life and practical.

References

[1] F. Delale, F. Erdogan, The crack problem for a nonhomogeneous plane, J. Appl. Mech. 50 (1983) 609–614.

[2] J.W. Eischen, Fracture of nonhomogeneous materials, Int. J. Fract. 34 (1987) 3–22.

[3] Ananda Thomas Khoirullah, et al,. Static Stress Analysis of Fork on Rubber Slab Lifting Aid using Finite Element Method. IJMEAS, (2024). Doi: 10.53893/ijmeas.v2i3.316

[4] Huu-Dien Nguyen, Shyh-Chour Huang, Using the Extended Finite Element Method to Integrate the Level-Set Method to Simulate the Stress Concentration Factor at the Circular Holes Near the Material Boundary of a Functionally-Graded Material Plate, JMR&T, 21C (2022) 4658-4673.

[5] L. Ma, L.-Z. Wu, L.-C. Guo, Z.-G. Zhou, Dynamic behavior of a finite crack in the functionally graded materials, Mech. Mater. 37 (11) (2005) 1153–1165.

[6] M. Naebe, K. Shirvanimoghaddam, Functionally graded materials: a review of fabrication and properties, Appl. Mater. Today 5 (2016) 223–245.

[7] Huu-Dien Nguyen, Use of XTFEM based on the consecutive interpolation procedure of quadrilateral element to calculate J-integral and SIFs of an FGM plate. T&AMF, Volume 127, October 2023, 103985.

[8] G.R. Irwin, J.M. Krafft, P.C. Paris, and A.A. Wells, "Basic Concepts of Crack Growth and Fracture," NRL Report 6598, Naval Research Laboratory, Washington, DC, (November 21, 1967).

[9] J. Sladek, V. Sladek, C. Zhang, An advanced numerical method for computing elastodynamic fracture parameters in functionally graded materials, Comput. Mater. Sci. 32 (2005) 532–543.

[10] Huu-Dien Nguyen, Shyh-Chour Huang, Designing and Calculating the Nonlinear Elastic Characteristic of Longitudinal–Transverse Transducers of an UltrasonicMedical Instrument Based on theMethod of Successive Loadings, Materials 15 (11), 4002, 2022.

[11] Nestor Perez, Fracture Mechanics, Kluwer Academic Publishers, (2004).

[12] Huu-Dien Nguyen, Shyh-Chour Huang, The Uniaxial Stress Strain Relationship of Hyperelastic Material Models of Rubber Cracks in the Platens of Papermaking Machines Based on Nonlinear Strain and Stress Measurements with the Finite Element Method, Materials, 2021

[13] L. Ma, J. Li, R. Abdelmoula, L.-Z. Wu, Dynamic stress intensity factor for cracked functionally graded orthotropic medium under time-harmonic loading, Eur. J. Mech. A. Solids 26 (2) (2007) 325–336.

[14] Ananda Thomas Khoirullah, Rachmat Dwi Sampurno. Static Stress Analysis of Fork on Rubber Slab Lifting Aid using Finite Element Method.(2024). Doi: 10.53893/ijmeas.v2i3.316

[15] J.D. Eshelby, "Calculation of Energy Release Rate," in Prospects of Fracture Mechanics, G.C. Sih, H.C. Von Elst, and D. Broek, Noordhoff, Growingen,(1974) 69-84.

[16] Riveros, G. A., and Gopalaratnam, V. S. Post-cracking behavior of reinforced concrete deep beams: A numerical fracture investigation of concrete strength and beam size. ASCE Structural Journal, (2005).

[17] Huu-Dien Nguyen. Using Matlab to Study of the Response of the System to Oscillatory Influences be an Oscillatory Effect on the Resting Antenna. International Journal of Multidisciplinary Research and Growth Evaluation, (2025).

[18] Huu-Dien Nguyen, Shyh Chour Huang. Calculating Strain Energy Release Rate, Stress Intensity Factor and Crack Propagation of an FGM Plate by Finite Element Method Based on Energy Methods. Materials, (2025).

[19]. Huu Dien Nguyen. Application of the eXtended Finite Element Method for Simulating Random Holes in Functionally Graded Plates. Materials Proceedings. (2025)

[20] Huu-Dien Nguyen. Extended Finite Element Approach for Simulating Arbitrary Openings in Functionally Graded Plates

. International Journal of Mechanics, Energy Engineering and Applied Science (IJMEAS), (2025).

[21]. Huu Dien Nguyen. Using the eXtended Finite Element Method (XFEM) to Simulate Own Frequency under External Influences of a Closed System based on Dynamic Compensation Method. Journal of International Multidisciplinary Research. (2025)

[22]. Huu Dien Nguyen, Shyh Chour Huang. Applying Quarter-Point Singular Element in Finite Element Method to Calculate J-Integral and Stress Intensity Factors of a Rectangular Isotropic FGM Plate. Materials. (2025)